Radial Vibration Measurement of Rotary Shafts through Electrostatic Sensing and Hilbert-Huang Transform

Lijuan Wang[a,b], Yong Yan[b], Yonghui Hu[a], Xiangchen Qian[a]
[a] School of Control and Computer Engineering
North China Electric Power University, Beijing 102206, P.R.China
[b] School of Engineering and Digital Arts
University of Kent, Canterbury, Kent CT2 7NT, U.K.

***Abstract*—Radial vibration measurement of rotary shafts plays a significant part in condition monitoring and fault diagnosis of rotating machinery. This paper presents a novel method for radial vibration measurement through electrostatic sensing and HHT (Hilbert-Huang Transform) signal processing. The foundational characteristics of the electrostatic sensor in the vicinity of a drifting shaft are studied through Finite Element Modelling. Experimental tests were conducted on a purpose-built test rig to characterize the operating condition of the rotor at different rotational speeds (400 rpm and 600 rpm). A normal working shaft and an eccentric shaft were tested and the output signals from the electrostatic sensors were analyzed. Through empirical mode decomposition (EMD) on the electrostatic signals, the intrinsic mode functions (IMF) including the vibration information of the shaft are identified and further analyzed in the time-frequency domain. Experimental results suggest that the electrostatic sensing technique in conjunction with HHT provides a simple and cost-effective approach to radial vibration measurement of rotary shafts.**

Keywords—radial vibration measurement; rotary shaft; electrostatic sensor; Finit Element Modelling; Hilbert-Huang Transform

I. INTRODUCTION

Rotary shafts are critical mechanical parts of rotating machinery and are commonly subject to mechanical vibration in industrial processes. In order to assess the health status and detect the potential malfunction of the working devices, reducing system downtime and associated cost, it is necessary to continuously and accurately monitor the vibration of the shaft system.

There are a variety of techniques available for vibration measurement, including measurement of displacement, velocity or acceleration [1]. Displacement transducers of the eddy-current type are commonly used to measure the relative motion between a shaft and its bearings, however, they do not work for dielectric rotors. Piezoelectric accelerometers are widely used for measuring absolute casing vibration and are possibly to obtain vibration velocity with integration [2]. Recently, a number of new methods have been proposed for shaft vibration detection. Rothberg et al applied a laser Doppler vibrometry to monitor the radial vibration of a rotor and analyzed the effects of surface roughness, instrument misalignments and pseudo-vibration on the performance of the measurement system [3]. Tong et al designed a reflective intensity-modulated non-contact optical fiber sensing system to detect radial vibration of high-speed rotating machinery [4]. Vyroubal estimated the vibration signature using optical sensors through spectral analysis of phase-modulated light pulses [5]. Okabe et al described an ultrasonic sensor based method for shaft vibration detection by measuring the propagation time of the ultrasonic wave from the sensor to the shaft surface [6]. However, the optical and acoustic sensors may not function well in hostile environments due to the presence of dust and background acoustic noise.

This paper presents a novel radial vibration measurement technique using electrostatic sensors and Hilbert-Huang Transform (HHT). Electrostatic sensing techniques have been successfully applied in multiphase flow measurement [7, 8] and condition monitoring of aero-engines [9, 10]. Recently, some research studies have investigated the application of electrostatic sensors to the operating speed measurement of mechanical devices, such as conveyor belt speed and rotor speed measurement [11,12]. The effectiveness of the proposed methods was verified through theoretical analysis and experimental tests. As a time-frequency analysis method, HHT outperforms the conventional Fast Fourier Transform (FFT), Wavelet Transform (WT) and Wigner-Ville distribution (WVD) in term of nonlinear and nonstationary signal processing [12]. Vibration signals from rotating machinery under malfunctions are commonly unstable and nonlinear, so HHT signal processing techniques are deployed in this study to measure the radial vibration of the rotary shafts. The output variations of electrostatic sensors under the condition of shaft vibration are investigated theoretically through Finite Element Modelling (FEM). In practice, the resulting signals from the electrostatic sensors are conditioned and decomposed into several modes. The vibration frequencies are identified and detected from the Hilbert-Huang spectra. Advantages of the proposed technique include non-contact sensing, simple structure, low cost, multi-functionality and suitability for applications in hostile environments.

II. Methodology of Radial Vibration Measurement

A. Measurment Principle

Fig. 1 shows the basic principle of the radial vibration measurement system using electrostatic sensors. When a shaft is in rotational motion, its surface becomes electrostatically charged due to the relative motion between the shaft surface and air. The insulated electrode with a suitable charge detection circuit is mounted in the vicinity of the shaft to detect the charge on the rotating surface. The signals are generated through electrostatic induction due to the moving surface with reference to the electrostatic sensor. In practice, the signals are random due to environmental factors (temperature and humidity), surface roughness of the shaft and installation effects of electrostatic sensors. However, the difference between a pair of sensor signals, such as S_1 and S_2, or S_3 and S_4, is able to indicate the drifting motion of the shaft. Because they are installed to monitor the same shaft under the same environmental conditions, the main factor which affects the signals' difference is the distance between the electrode and the shaft. As shown in Fig.1, once the shaft has radial vibration, i.e. the rotating center changes from *O* to *O'*, sensors 1 and 3 will detect more significant signal amplitude due to the closer distance between the shaft and the electrodes. Meanwhile, sensors 2 and 4 yield lower signal amplitude. Since the original signal from the electrode is extremely weak, a high-performance signal conditioning unit is utilized, which comprises a current-to-voltage convertor, pre-amplifier, secondary amplifier and low-pass filter. Through realizing the algorithms for the extraction of the vibration parameters in a signal processing unit, the vibration frequency is determined.

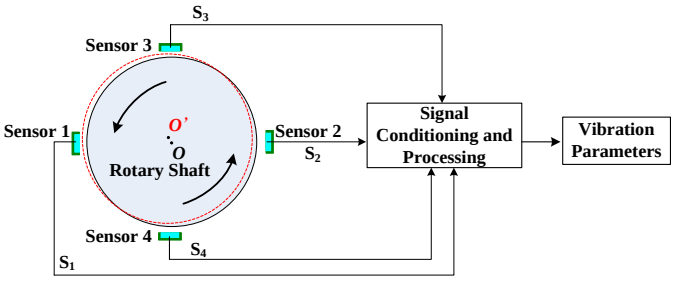

Fig. 1. Principle of radial vibration measurement using electrostatic sensors.

B. Finite Element Model

Finite Element Modelling techniques are applied to study the characteristics of the electrostatic sensor that is installed for the monitoring of a vibrating shaft. In the FEM modelling (see Fig. 2) two electrostatic electrodes are placed on the opposite sides of the shaft with a distance of 4 mm away from the shaft surface. Each electrode is a copper strip of 20 mm in length and 3 mm in width. The shaft is made of PTFE (Polytetrafluoroethene) with a diameter of 60 mm. It is assumed that electrostatic charge is evenly distributed on the motor surface with a charge density of -1 μ C/m^2. The air is assumed to have a dielectric constant of 1.

The electrostatic field in the modelling can be described using Poisson's equation and corresponding boundary condition:

$$\begin{cases} -\nabla\cdot\left(\varepsilon_0\varepsilon_r\nabla V\right)=\rho \\ V_E=0, V_B=0 \end{cases} \quad (1)$$

where ε_0 is the permittivity of free space, ε_r the relative permittivity of the media (air in this case), V the electrical potential and ρ the space charge density. The electrical potential of the electrode and boundary (V_E and V_B) is set to 0 as the boundary conditions.

The total charge induced on the electrode is obtained through surface integration of charge density. Fig. 3 plots the computational results within one revolution under three different conditions. The first case is normal rotation, which means no vibration exists during rotational motion. The second case is that the rotational axis is drifting to the direction of sensor 1 and O' is 0.5 mm away from the geometric centre *O*, i.e. S = 0.5 mm. The third case is that distance between O' and *O* is extended to 1 mm, i.e. S = 1 mm. As shown in Fig. 3, the electrostatic charge levels from sensors 1 and 2 are both maintaining at around 0.57 *nC* under normal working conditions. As the shaft drifting closer to sensor 1, the signal amplitude increases while the charge level of sensor 2 decreases due to the larger distance to the rotating shaft. Moreover, the signals reach the maximum and minimum values, respectively, when the rotational angle of the shaft α (see Fig. 2(b)) is π and then gradually return to the original levels.

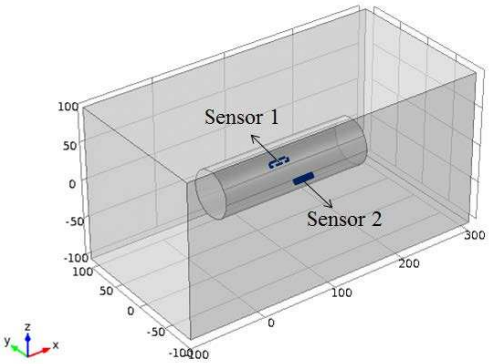

(a) Structure of the model

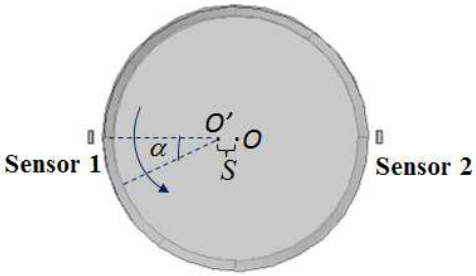

(b) Installation of electrostatic sensors

Fig. 2. FEM of the radial vibration measurment system.

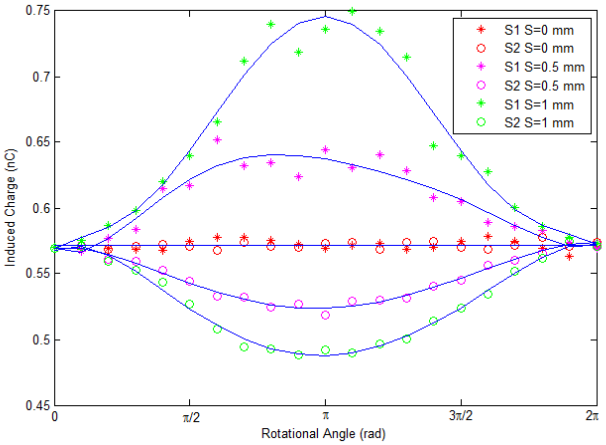

Fig. 3. Induced charge on the electrostatic sensors under different conditions.

C. Hilbert-Huang Transform

In reality, the electrostatic charge is unevenly distributed on the shaft surface due to the roughness of surface, environmental factors and so on. The drift of the shaft is not just in the horizontal direction and can be a combined effect of horizontal and vertical drifts. Additionally, the noise from electronic circuits and operating conditions may affect the output signals of electrostatic sensors. In most cases, the vibration of a rotational device is not a stationary process. In order to identify and extract the vibration features from complex signals, an effective time-frequency analysis method, Hilbert Huang Transform, is considered as a most suitable method to process the signals in this study.

HHT comprises empirical mode decomposition (EMD) and Hilbert transform [13-15]. Firstly, the time-series signal $s(t)$ is decomposed into a number of intrinsic mode functions (IMFs) $c(t)$ and a residual $r(t)$ through a sifting process:

$$s(t) = \sum_{i=1}^{n} c_i(t) + r(t) \tag{2}$$

Then the Hilbert transform is applied to each IMF to obtain a complex representation of IMF,

$$d_i(t) = \frac{1}{\pi} P \int_{-\infty}^{\infty} \frac{c_i(\tau)}{t-\tau} d\tau \tag{3}$$

where P indicates the Gauchy principle value. An analytical signal $z_i(t)$ can be constructed by

$$z_i(t) = c_i(t) + jd_i(t) = a_i(t)e^{j\theta_i(t)} \tag{4}$$

where the amplitude $a_i(t)$ and the phase $\theta_i(t)$ are determined by

$$a_i(t) = \sqrt{(c_i(t))^2 + (d_i(t))^2} \tag{5}$$

$$\theta_i(t) = \arctan\left(\frac{d_i(t)}{c_i(t)}\right) \tag{6}$$

Finally, the instantaneous frequency $\omega_i(t)$ of each IMF is defined as

$$\omega_i(t) = \frac{1}{2\pi} \cdot \frac{d\theta_i(t)}{dt} \tag{7}$$

The time-frequency distribution of the amplitude is referred to as Hilbert spectrum:

$$H(\omega, t) = \mathrm{Re}\left(\sum_{i=1}^{n} a_i(t) e^{j\int \omega_i(t)dt}\right) \tag{8}$$

where n is the number of IMFs. The marginal spectrum can be defined as

$$h(\omega) = \int_0^T H(\omega, t)dt \tag{9}$$

where T is the total data length. The contribution of the total amplitude from each frequency is represented by the marginal spectrum.

III. Experimental Results and Discussion

A. Test Conditions

A vibration test rig was designed and implemented. Fig. 4 shows the experimental rig that was used to conduct the tests in this study. The rotor is driven by a three-phase asynchronous motor through a coupling. The rotational speed of the motor is adjustable from 0 to 3000 rpm through the motor controller. Two PTFE shafts with a diameter of 60 mm were tested. One is a normal shaft while the other is eccentric with S = 1 mm. A pair of electrostatic sensors was placed 4 mm away from the shaft surface. The electrode in each electrostatic sensor is made of copper in a form of a wide track on a small piece of printed circuit board (PCB). The electrode is 20 mm long and 3 mm wide. To ensure high signal-to-noise ratio the electrode is attached directly to the current-to-voltage convertor and pre-amplifier of the signal conditioning unit, which converts and amplifies the current signal in the order of 10 nA to a voltage signal in the order of 100 mV. The voltage gain of the secondary amplifier used in this test is 10. HHT algorithm is realized in the signal processing unit. All the tests were conducted under ambient temperature of 21.8°C and relative humidity of 44%.

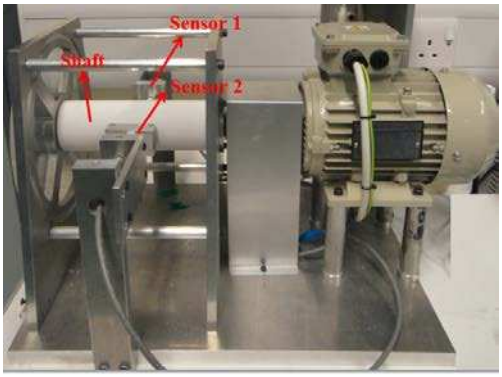

Fig. 4. Test rig for radial vibration measurement.

B. Signal Processing and Analysis

Figs. 5 and 6 depict the signals from the two sensors at the speed of 400 rpm and 600 rpm, respectively. It can be seen that the amplitudes of the two signals (S_1 and S_2) remain the same level during the rotational motion for the normal shaft. While the signals from the eccentric shaft (S_1' and S_2') fluctuate significantly due to the variable distance from the rotating shaft to the sensors. Between the two signals S_1' and S_2', there is

clearly a phase shift, which originates from the symmetric installation of the two sensors. Meanwhile, the maximum peak of S_1' and the minimum peak of S_2' are not symmetric about the X axis, because the rotating centre is 1 mm away from the geometric centre of the eccentric shaft. This indicates the shaft is drifting towards sensor 1 and verifies the modelling results in Fig. 3. As shown in Figs. 5 and 6, the signal amplitude increases with the rotational speed.

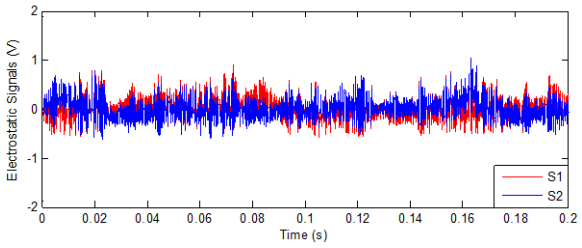

(a) Electrostatic signals from the normal shaft

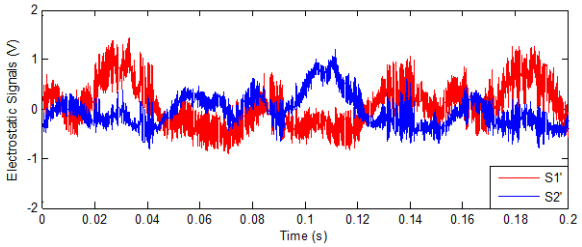

(b) Electrostatic signals from the eccentric shaft

Fig. 5 Electrostatic signals at the speed of 400 rpm.

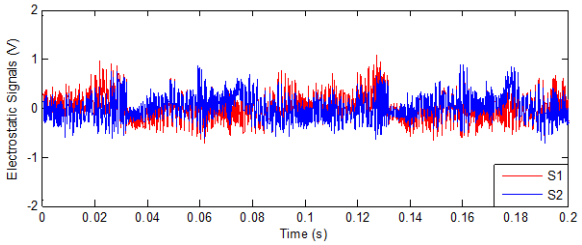

(a) Electrostatic signals from the normal shaft

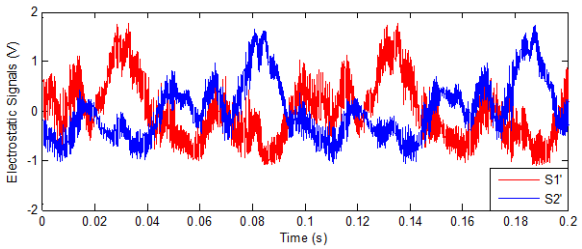

(b) Electrostatic signals from the eccentric shaft

Fig. 6 Electrostatic signals at the speed of 600 rpm.

The sensor signals are processed through Hilbert-Huang transform. For each signal waveform, 9 IMFs are obtained with different frequency ranges. The marginal spectra of S_1 and S_2 (Fig. 7) show the dominant frequency at the speed of 600 rpm is exactly the rotating frequency (f = 600 rpm/60 = 10 Hz) for the normal shaft. The eccentric shaft has elevated the amplitude of the rotational frequency and generated the visible harmonic components of at 2*f*. Fig. 8 shows the Hilbert-Huang spectra of S_1, S_2, S_1' and S_2'. It is clear that the dominant energy concentrates around the rotational frequency (the strong red streaks in the spectra). Some periodic waves just above the main rotational frequency are visible in the spectra, which indicate the vibration effects of the shafts. The spectra also show that a range of other frequency components are present due to the noise in the signal conditioning electronics and the remaining structural instability of the test rig.

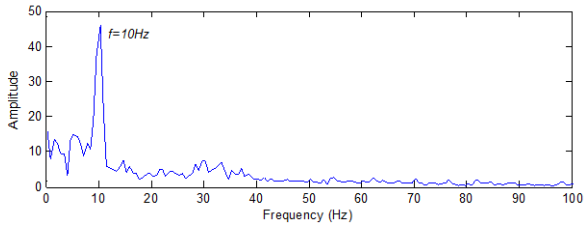

(a) Marginal spectrum of S_1

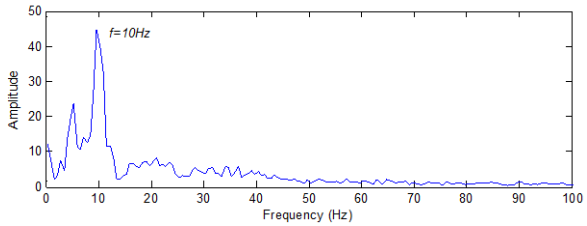

(b) Marginal spectrum of S_2

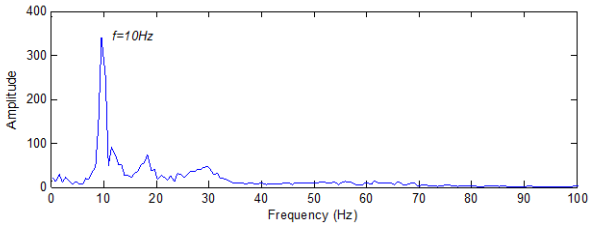

(c) Marginal spectrum of S_1'

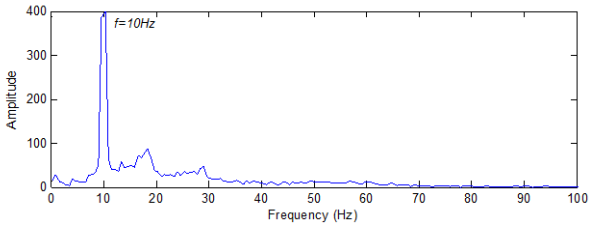

(d) Marginal spectrum of S_2'

Fig. 7 Marginal spectra of signals at the speed of 600 rpm.

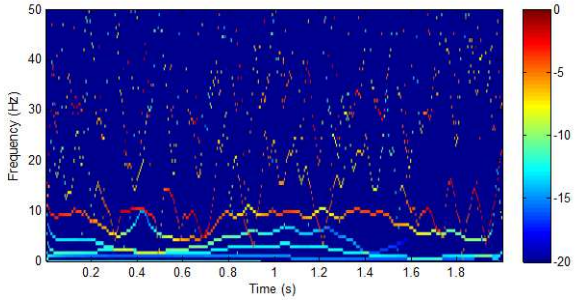

(a) Hilbert-Huang spectrum of S_1

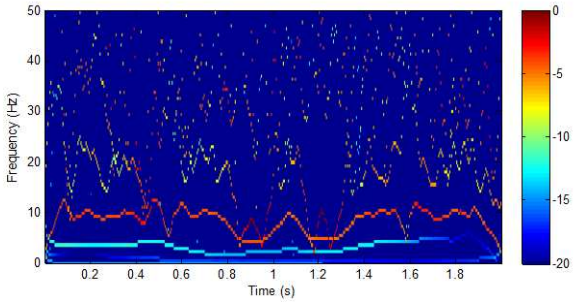

(b) Hilbert-Huang spectrum of S_2

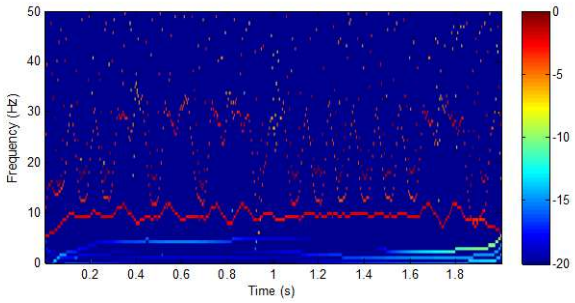

(c) Hilbert-Huang spectrum of S_1'

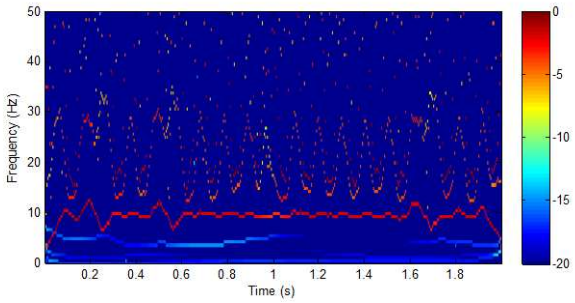

(d) Hilbert-Huang spectrum of S_2'

Fig. 8 Hilbert-Huang spectra of signals at the speed of 600 rpm.

IV. Conculsions

The FEM model of electrostatic sensors has been established to study the sensing characteristics under rotary and vibratory motion of the shaft. The assumption that output of the electrostatic sensors contains vibration information of the shaft has been verified through the FEM analysis. Meanwhile, experimental investigations have been conducted to obtain the real signals from the sensors when the shaft is in normal or eccentric motion. HHT techniques have been applied to identify and extract the vibration features from the sensor signals. Results presented have demonstrated that the waveforms from the eccentric shaft fluctuate more significantly than the normal signals. The higher amplitude of the signal can be used to indicate the shaft is drifting in the direction where the sensor is installed. The HHT analysis has indicated that the eccentric shaft not only raises the rotating frequency but also introduces the harmonic frequency components. Further research will be conducted on fault identification and diagnosis for rotary shaft systems.

Acknowledgment

The authors wish to acknowledge the National Natural Science Foundation of China (No. 51375163), the Chinese Ministry of Science and Technology (No. 2012CB215203), the Chinese Ministry of Education (No. B13009) for providing financial support for this research. Lijuan Wang would like to thank the IEEE Instrumentation and Measurement Society for 2015 Graduate Fellowship Award.

References

[1] M. L. Adams, Rotating machinery vibration: From analysis to troubleshooting, CRC Press, 2010.

[2] R. B. Randall, “State of the art in monitoring rotating machinery-Part 1”, Sound Vib., vol. 38, no. 3, pp. 14-21, 2004.

[3] S. J. Rothberg, B. J. Halkon, M. Tirabassi and C. Pusey, “Radial vibration measurements directly from rotors using laser vibrometry: The effects of surface roughness, instrument misalignments and pseudo-vibration,” vol. 33, no. , pp. 109-131, Nov. 2012.

[4] Q. Tong, H. Ma, L. Liu, X. Zhang and G. Li, “Key technology study on radial vibraition system of high-speed rotating machinery,” Chinese Journal of Scientific Instrment, vol. 5, no. 32, pp. 1026-1032, May 2011.

[5] D. Vyroubal, “Optical method for instant estimate of vibration signature based on spectrum analysis of phase-modulated light pulses,” IEEE Trans. Instrum. Meas., vol. 53, no. 1, pp. 181-185, Feb. 2004.

[6] S. Okabe and S. Tanaka, “Measurement of shaft vibration using ultrasonic sensor,” in Proc. of SICE 2003 Annual Conference, pp. 1155-1158, Fukui, Japan, Aug. 2003.

[7] Y. Yan, B. Byrne, S. Woodhead and J. Coulthard, “Velocity measurement of pneumatically conveyed solids using electrodynamic sensors,” Meas. Sci. Technol., vol. 6, no. 6, pp. 515-537, Dec. 1995.

[8] X. Qian and Y. Yan, “Flow measurement of biomass and blended biomass fuels in pneumatic conveying pipelines using electrostatic sensor-arrays,” IEEE Trans. Instrum. Meas., vol. 61, no. 5, pp. 1343-1352, Jan. 2012.

[9] J. E. Booth, T. J. Harvey, R. J. K. Wood and H. E. G Powrie, “Scuffing detection of TU3 cam–follower contacts by electrostatic charge condition monitoring,” Tribol. Int., vol. 43, no. 1-2, pp. 113-128, Jan. 2010.

[10] T. J. Harvey, R. J. K. Wood and H. E. G. Powrie, “Electrostatic wear monitoring of rolling element bearings,” Wear, vol. 263, no. 7-12, pp. 1492-1501, Sep. 2007.

[11] Y. Hu, L. Wang, X. Wang, X. Qian and Y. Yan, “Simultaneous measurement of conveyor belt speed and vibration using an Electrostatic sensor array,” in Proc. of IEEE International Instrumentation and Measurement Technology Conf., pp.757-761, Pisa, Italy, 11-14 May 2015.

[12] L. Wang, Y. Yan, Y. Hu and X. Qian, “Rotational speed measurement through electrostatic sensing and correlation signal processing,” IEEE Trans. Instrum. Meas., vol. 63, no. 5, pp. 1190-1199, Dec. 2013.

[13] N. E. Huang, Z. Shen, S. R. Long, M. C. Wu, H. H. Shih, Q. Zheng, N. Yen, C. C. Tung and H. H. Liu, “The empirical mode decomposition and the Hilbert spectrum for nonlinear and non-stationary time series analysis,” in Proc. of the Royal Society of London, vol. 454, no. 1971, pp. 903-995, Mar. 1998.

[14] W. Zhang, C. Wang and H. Wang, “Hilbert–Huang Transform-Based electrostatic signal analysis of ring-shape electrodes with different widths,” IEEE Trans. Instrum. Meas., vol. 61, no. 5, pp. 1209-1216, May 2012.

[15] H. Ding, Z. Huang, Z Song and Y. Yan, “Hilbert–Huang transform based signal analysis for the characterization of gas–liquid two-phase flow,” Flow Meas. Instrum., vol.18, no.1, pp. 37-46, Mar. 2007.